https://doi.org/10.5194/tc-2021-211
Preprint. Discussion started: 27 September 2021

The Cryosphere Discussions

Evaluating sources of an apparent cold bias in MODIS land surface temperatures in the St. Elias Mountains, Yukon, Canada

Ingalise Kindstedt[1], Kristin M. Schild[1,2], Dominic Winski[1,2], Karl Kreutz[1,2], Luke Copland[3], Seth Campbell[1,2], and Erin McConnell[1]

[1]Climate Change Institute, University of Maine, Orono, Maine, USA
[2]School of Earth and Climate Sciences, University of Maine, Orono, Maine, USA
[3]Department of Geography, Environment and Geomatics, University of Ottawa, Ottawa, Ontario, Canada

Correspondence: Ingalise Kindstedt (ingalise.kindstedt@maine.edu)

Abstract. Remote sensing data are a crucial tool for monitoring climatological changes and glacier response in areas inaccessible for in situ measurements. The Moderate Resolution Imaging Spectroradiometer (MODIS) land surface temperature (LST) product provides temperature data for remote glaciated areas where weather stations are sparse or absent, such as the St. Elias Mountains (Yukon, Canada). However, MODIS LSTs in the St. Elias Mountains are offset from available weather station measurements, showing an apparent cold bias, the source of which is unknown. Here, we show that the MODIS offset likely results from the occurrence of near-surface temperature inversions rather than from the MODIS sensor's large footprint size or from poorly constrained snow emissivity values used in LST calculations. We find that an offset in remote sensing temperatures is present not only in MODIS LST products, but also in Advanced Spaceborne Thermal Emissions Radiometer (ASTER) and Landsat temperature products, both of which have a much smaller footprint (90-120 m) than MODIS (1 km). In all three datasets, the offset was most pronounced in the winter (mean apparent cold bias >8°C), and least pronounced in the spring and summer (mean apparent cold bias <2°C). We also find this enhanced seasonal offset in MODIS brightness temperatures, before the incorporation of snow surface emissivity into the LST calculation. Finally, we find the MODIS LST offset to be consistent in magnitude and seasonal distribution with modeled temperature inversions, and to be most pronounced under conditions that facilitate near-surface inversions, namely low incoming solar radiation and wind speeds, at study sites Icefield Divide (60.68°N, 139.78°W, 2,603 m a.s.l) and Eclipse Icefield (60.84°N, 139.84°W, 3,017 m a.s.l.). These results demonstrate that efforts to improve the accuracy of MODIS LSTs should focus on understanding near-surface physical processes rather than refining the MODIS sensor or LST algorithm. In the absence of a physical correction for the offset, we apply a statistical correction, enabling the use of mean annual MODIS LSTs to qualitatively and quantitatively examine temperatures in the St. Elias Mountains and their relationship to melt and mass balance.

1 Introduction

In recent decades, the Arctic has warmed at a more rapid rate than the rest of the planet, with far reaching impacts (Winton, 2006; Serreze and Barry, 2011; You et al., 2021). In particular, the loss of Arctic glaciers has reduced the Earth's albedo, further accelerating warming, and contributed to global sea level rise (Serreze and Barry, 2011; Zemp et al., 2019; Hugonnet

https://doi.org/10.5194/tc-2021-211
Preprint. Discussion started: 27 September 2021

et al., 2021). The St. Elias mountains are situated on the border of Alaska and the Yukon in a region experiencing pronounced warming and glacier mass loss compared to the rest of the Arctic (Farinotti et al., 2019; Zemp et al., 2019; Hugonnet et al., 2021). Alaskan glaciers alone have contributed over 25% of observed sea level rise to date, the largest contribution of any one glaciated region, excluding the Greenland and Antarctic Ice Sheets (Zemp et al., 2019; Hugonnet et al., 2021). Additionally, Alaskan glaciers are losing mass at some of the highest rates globally ($-66.7\ \mathrm{Gt\,yr^{-1}}$), and therefore remain a matter of critical importance for sea level prediction (Hugonnet et al., 2021). The greater North Pacific cordillera contains over 40 mm of global sea level rise in a combination of large icefields and small alpine glaciers (Farinotti et al., 2019). Therefore, widespread monitoring of glacier mass changes in the North Pacific cordillera is particularly crucial even among glaciated alpine regions.

Glacier mass changes are driven by changes in the surface energy balance; in effect, glacier mass loss is largely controlled by atmospheric warming (Cuffey and Paterson, 2010). In order to better predict the impacts of continued atmospheric warming, we need to be able to monitor temperature change and glacier response. However, due to the inaccessibility of much of the Arctic for in situ measurements, our understanding of the region's climatic behavior relies heavily on remote sensing products, such as Moderate Resolution Imaging Spectroradiometer (MODIS) land surface temperatures (LSTs). Temperatures derived using remote sensing techniques are definitionally not measured directly. Instead, they are inferred from measurements taken by satellite sensors of the energy emitted by the earth's surface. Remote sensing temperatures include the final surface temperature product, as well as "brightness temperature", an intermediate temperature product used to produce the final surface temperature. In contrast, temperatures measured in situ are directly measured using instruments onsite, and can be measured for both the earth's surface and the air above it. Unless otherwise stated, all in situ temperatures used in this study are taken for the air $\sim 2\ \mathrm{m}$ above the land surface. Instrumentation for both remote sensing and in situ temperatures used here is discussed below. A summary of the temperatures used in this study is shown in Table 1. MODIS LSTs are a valuable tool for monitoring climate in remote regions because of their high temporal resolution and long temporal record; they provide two decades of near-daily imagery under clear-sky conditions. However, MODIS LSTs have been observed to be lower than in situ surface and air temperatures at a number of snow- and ice-covered sites. For example, at Summit, Greenland, 2008-2009 MODIS LSTs were an average of 5.5°C lower than coincident $2\ \mathrm{m}$ air temperatures, amounting to an $\sim$3°C apparent cold bias in the MODIS LSTs once the difference between surface and air temperatures was accounted for (Koenig and Hall, 2010). Likewise, in Svalbard, wintertime MODIS LSTs from a snow-covered permafrost site showed an apparent cold bias of 1.5°C to 6°C (mean = 3°C) relative to in situ surface temperatures (Westermann et al., 2012), and MODIS LSTs from the Austfonna ice cap during 2004-2011 showed an apparent cold bias relative to both in situ surface (RMSE = 5.3°C) and air (RMSE = 6.2°C) temperatures (Østby et al., 2014). In this study, we focus on an observed offset in MODIS LSTs from automated weather station (AWS) temperatures in the glaciated Upper Kaskawulsh-Donjek region of the St. Elias Mountains (Yukon, Canada; hereafter referred to as "St. Elias"). In this region, average daily MODIS LSTs were shown to be colder than downscaled and observed temperatures by 5–7°C when snow cover was >90% (Williamson et al., 2017). Remote sensing temperature products are especially crucial for relating glacier behavior and mass balance to climatological changes in rugged alpine regions where glaciers tend to be at higher elevations than most nearby weather stations. Our study sites in the St. Elias are located above 2,500 m a.s.l., while nearby Environment and Climate Change Canada weather stations are located at 610 m a.s.l. (Haines

https://doi.org/10.5194/tc-2021-211
Preprint. Discussion started: 27 September 2021


The Cryosphere Discussions

Table 1. Temperatures used in this study. Type of temperature is shown by rows. Measurement technique is shown by columns.

	In Situ	Remote Sensing
Air Temperatures	AWS iButton	
Surface Temperatures		MODIS LST ASTER surface temperature
Brightness Temperatures (BT)		MODIS BT ASTER BT Landsat BT

Junction) and 806 m a.s.l. (Burwash Landing; Fig. 1). Lower elevation sites receive moisture from different air masses and are sensitive to different sources of variability than their high elevation counterparts, so data from these stations are not necessarily representative of climatic behavior at glaciated alpine sites (McConnell, 2019). In particular, low elevation sites are primarily sensitive to local climate, while higher elevation sites are sensitive to atmospheric circulation patterns on a large spatial scale (e.g. Alaska Range-central tropical Pacific teleconnections, Winski et al. 2018). Additionally, low-elevation weather stations likely underestimate the warming experienced at nearby higher elevation sites. Modeling studies (Chen et al., 2003; Giorgi et al., 1997) predict that warming rates increase with elevation, a prediction that is borne out by observation in a number of alpine mountain ranges including the St. Elias and greater North Pacific cordillera (high elevation sectors of Alaska and parts of the Yukon and British Columbia; Williamson et al., 2020; Diaz et al., 2014; Pepin et al., 2015; Rangwala and Miller, 2012).

Because we lack paired in situ surface and air temperature measurements in the St. Elias, it is not clear whether the MODIS LST offset in the region results from the instrumentation and algorithm used to produce MODIS LSTs or whether it is a real temperature difference between the air and surface. Unlike weather stations, which measure air temperature at a point typically 2 m above the surface, MODIS LSTs record the temperature of the surface itself across a 1 km^2 grid cell. Although air temperature and surface temperature are closely related, they are distinct and their response to the same forcing can differ (Jin and Dickinson, 2010). During the production of MODIS LSTs, clouds and blowing snow can produce low temperatures if they are erroneously categorized as the land surface (Westermann et al., 2012). Without accurate cloud masking, apparent cold biases in MODIS LSTs have been previously observed at Summit, Greenland in both summer (∼3°C; Koenig and Hall, 2010) and winter (∼5°C; Shuman et al., 2014). However, the cloud mask has since been updated to address this problem (Yao et al., 2020). Apparent cold biases at Summit have also been attributed to near-surface temperature inversions (Adolph et al., 2018). Near-surface temperature inversions occur when the surface is colder than the air directly above it and develop over glaciated regions when heat transfer from the surface to the air occurs as a result of an energy imbalance at the surface-air interface (Adolph et al., 2018). Under low incoming solar radiation, upward longwave radiation emitted by the surface must be almost completely balanced by downward longwave radiation emitted by the atmosphere (Hudson and Brandt, 2005). Because the

https://doi.org/10.5194/tc-2021-211
Preprint. Discussion started: 27 September 2021

The Cryosphere Discussions
Open Access
EGU

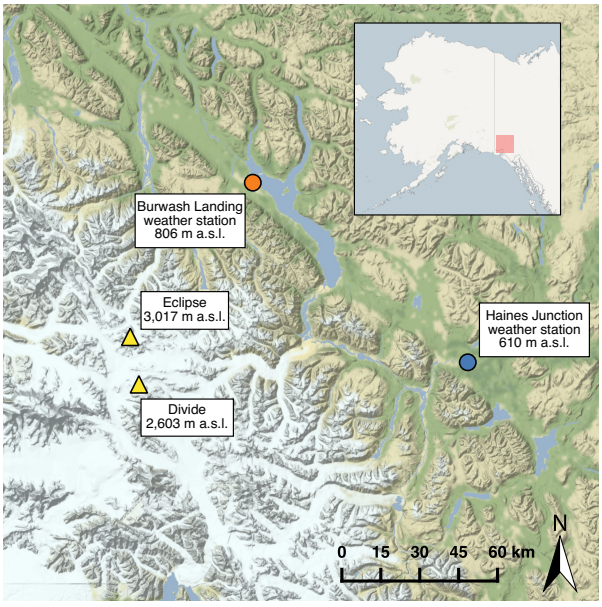

Figure 1. Study sites Eclipse and Divide (yellow triangles) and nearby weather station locations at Burwash Landing (orange circle) and Haines Junction (blue circle).

snow surface is a more efficient emitter than the atmosphere, the surface must cool relative to the air above it for the energy fluxes to balance (Hudson and Brandt, 2005). One hypothesis for the offset in MODIS LSTs in the St. Elias is the presence of near-surface temperature inversions similar to those observed at Summit. However, unlike the interiors of large ice sheets, alpine environments are characterized by heterogeneity in surface type, elevation, aspect, incline, wind scouring, and shading (note the many ridges and nunataks shown in Fig. 2), all of which affect surface energy balance. Conditions from Summit therefore cannot be used to infer near-surface temperature inversions in the St. Elias, and to our knowledge, such inversions have not to date been observed in other alpine regions. Here, we both test alternative hypotheses to explain the offset in MODIS LSTs in the St. Elias and evaluate the plausibility of near-surface temperature inversions in the region.

First, the LST offset could result from the large (1 x 1 km) footprint of the MODIS sensor. The heterogeneity of the St. Elias' environment (surface type, elevation, aspect, incline, wind scouring, shading) may not be well represented by the average temperature value of a MODIS pixel. A second cause of the LST offset could be incorrect definition of emissivity values used to calculate MODIS LSTs from brightness temperatures. Since snow does not emit radiation uniformly, emissivity is not uniform across snow surface types, particularly in locations such as the St. Elias icefields, where compaction processes and surface melt occur heterogeneously over the variable terrain (Hori et al., 2006; Hulley et al., 2014; Shea and Jamieson, 2011). Therefore, the icefields undergo disparate changes in emissivity over hours to days, meaning that identifying a single representative emissivity value is challenging. Lastly, it may be that the LST offset does not arise during the calculation of

https://doi.org/10.5194/tc-2021-211
Preprint. Discussion started: 27 September 2021

The Cryosphere Discussions
Open Access
EGU

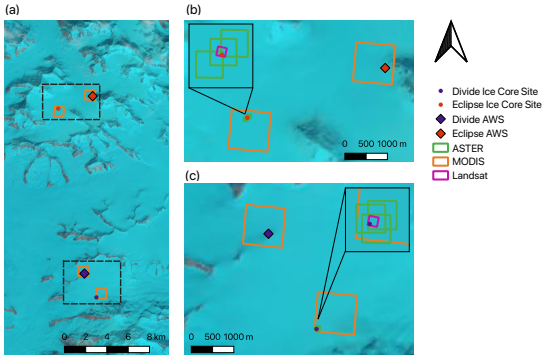

Figure 2. MODIS (orange box), ASTER (green box), and Landsat (pink box) footprints at Eclipse and Divide ice core and AWS sites. a) Upper Kaskawulsh-Donjek area containing Eclipse and Divide sites, b) Eclipse ice core (red dot) and AWS (red diamond) sites, c) Divide ice core (blue dot) and AWS (blue diamond) sites. Dashed lines in panel (a) show extents of panels (b) and (c). Background imagery from Landsat 8 on June 30, 2017.

LSTs at all, but is a real physical temperature difference between the surface and air due to the developement of a near-surface temperature inversion.

Our goal in this study is to determine whether the dominant source of the offset in MODIS LSTs from AWS temperatures at glaciated sites in the heterogeneous alpine environment of the St. Elias arises from (a) the large spatial footprint of the MODIS sensor in highly heterogeneous alpine terrain, (b) poorly constrained snow emissivity values, or (c) a real temperature difference between the surface and air due to near-surface temperature inversions. Since prior work has been unable to fully evaluate the apparent MODIS cold bias in alpine environments due to data limitations, the relative importance of competing hypotheses is unknown. Additionally, near-surface temperature inversions have to date only been studied on the major ice sheets, and their applicability to alpine environments remains untested. Here, we use two decades of overlapping MODIS and AWS measurements from the St. Elias to resolve some of these uncertainties and develop a correction factor for use in similar environments that lack AWS data. The AWS record from Divide is, to our knowledge, the longest such record from a glaciated high alpine area outside the European Alps. Importantly, Alaska is a much more influential region than the European Alps from a glacier mass balance perspective. During the period from 2000-2019, Alaskan glaciers lost mass at a rate of 66.7 $\mathrm{Gt\,yr^{-1}}$ in comparison to a rate of less than 4 $\mathrm{Gt\,yr^{-1}}$ in the European Alps. This work is therefore novel in its pairing of the Divide AWS temperature record with MODIS LSTs in an understudied system (glaciated high alpine regions) where we often rely solely on remote sensing data for temperature information, as well as in a location with severe consequences in terms of ice mass loss.

https://doi.org/10.5194/tc-2021-211
Preprint. Discussion started: 27 September 2021

The Cryosphere Discussions
Open Access
EGU

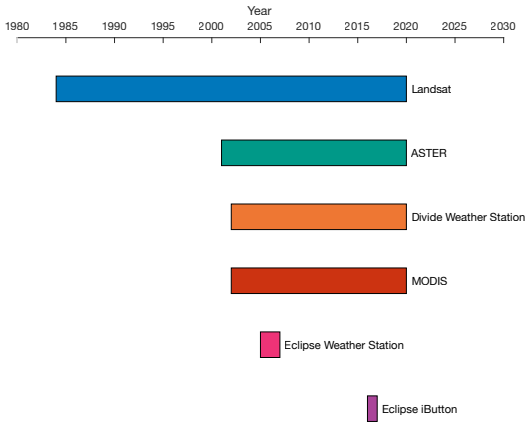

Figure 3. Temporal coverage of datasets used in this study. Time periods covered are 1984-present (Landsat), 2001-present (ASTER), 2002-present (Divide weather station), 2002-present (MODIS), 2005-2007 (Eclipse weather station), and 2016-2017 (Eclipse iButton).

2 Methods

2.1 Study sites and in situ data

In situ and MODIS temperature data were collected at study sites Eclipse Icefield (60.84° N, 139.84° W, 3,017 m a.s.l.; hereafter referred to as "Eclipse"), and Icefield Divide (60.68° N, 139.78° W, 2,603 m a.s.l.; hereafter referred to as "Divide"; Fig. 1) in the St. Elias Mountains. In situ temperatures at Divide were obtained from two adjacent AWS located on small nunataks, the first of which used a Campbell 107F temperature probe ($\pm$ 0.2°C) housed inside a solar radiation shield, which recorded hourly readings from 2002-2015. The second AWS was located ~300 m from the first, and recorded hourly temperatures with a HOBO S-THB-M008 12-bit sensor ($\pm$ 0.21°C) housed inside a solar radiation shield from 2009-present (Fig. 3). Both sensors at Divide were located ~2m above the surface. Temperatures at Eclipse were obtained from an AWS from 2005-2007, and a Maxim Integrated iButton Data Logger DS1922L ($\pm$ 0.5°C) from 21 May 2016 to 17 May 2017 (Fig. 3). The iButton recorded temperatures at 3-hour intervals and was placed inside a plastic container on a bedrock outcrop ~3 km from the site of an ice core drilled at Eclipse in 2016. We combine the Eclipse AWS and iButton datasets, as the temperature values recorded by each instrument were consistent. We refer to both the Divide AWS and the combined Eclipse iButton and AWS data as "AWS" for the remainder of this paper.

2.2 MODIS data

In this assessment of possible sources for the MODIS LST offset, we use the MODIS MYD21 LST product. The MOD21 and MYD21 (together referred to as MxD21) products employ an improved method for retrieving and assigning emissivity values compared to the MxD11 products previously examined (Williamson et al., 2017; McConnell, 2019), and have been shown to

https://doi.org/10.5194/tc-2021-211
Preprint. Discussion started: 27 September 2021

The Cryosphere Discussions

Table 2. Mean and standard deviation of differences between MODIS LSTs at the Divide ice core and AWS sites, median MODIS LST offsets by season at Divide and Eclipse, median MODIS brightness temperature (BT) offsets by season at Divide and Eclipse, and median calculated temperature inversions with surface emissivities of 0.95 and 0.99. Differences between MODIS LSTs at the ice core site and AWS site are reported as ice core site − AWS site (°C). All offsets are reported as MODIS − AWS (°C). Brightness temperatures for bands 31 and 32 are averaged together. Inversions are reported as negative values.

	Ice Core Site − AWS Site (°C)		MODIS LST − AWS (°C)		MODIS BT − AWS (°C)		$T_{surface} - T_{air}$(°C)	
Season	Mean	Std	Divide	Eclipse	Divide	Eclipse	$\epsilon_s = 0.95$	$\epsilon_s = 0.99$
Spring (MAM)	0.77	1.44	−0.68	−1.73	−1.74	−2.77	7.95	7.46
Summer (JJA)	1.16	0.77	−0.98	−1.12	−2.43	−2.53	0.73	0.65
Fall (SON)	−0.41	2.64	−4.43	−5.20	−5.64	−5.67	2.34	1.03
Winter (DJF)	−0.80	2.95	−8.40	−8.93	−9.39	−9.41	−7.14	−9.70

correct for MxD11 apparent cold biases over barren, but not glaciated, surfaces (Hulley, 2017; Li et al., 2020; Yao et al., 2020). MOD21 LSTs were not included in this study as the product was discontinued due to an optical crosstalk issue in the infrared bands (Hulley, 2017), therefore we focus solely on MYD21 LST data.

Our goal is to determine the dominant source of the offset in MODIS LSTs at glaciated sites in the St. Elias. Because the Eclipse and Divide AWS are located on nunataks, we test for the LST offset using MODIS data encompassing adjacent ice core sites ∼3 km from each AWS location, thereby excluding the dark nunatak surface from the MODIS pixel and focusing on the ice surface (Fig. 2). MODIS data at the Divide AWS nunatak and adjacent ice core site has a mean temperature difference of 0.27°C and standard deviation of 2.20°C. The difference between the two sites shows greater variability in the fall (std = 2.64) and winter (std = 2.95) than in the spring (std = 1.44) and summer (std = 0.77), with the ice core site tending to be slightly colder (mean winter temperature difference of -0.80°C). This may be due to the inclusion of the warmer nunatak surface in the MODIS pixel at the AWS site. Temperature differences between the Divide AWS and ice core site are summarized in Table 2. MODIS LST data were obtained for the period 2000-2020 (https://lpdaacsvc.cr.usgs.gov/appeears/) for dates with minimal cloud cover and a viewing angles < 30°, to mitigate the effect of viewing angle on temperature and emissivity. At Divide, 742 MODIS images taken between 11:00 a.m. and 1:30 p.m. were analyzed. Seasonally, 203 images were acquired in spring (MAM), 169 in summer (JJA), 188 in fall (SON), and 182 in winter(DJF). The average time between scenes at Divide was ∼9 days after filtering. At Eclipse, 100 MODIS images taken between 11:00 a.m. and 1:30 p.m. were analyzed. Seasonally, 25 images were acquired in spring, 24 in summer, 29 in fall, and 22 in winter. The average time between scenes at Eclipse was ∼43 days after filtering. A small number of summer MODIS LST offset results were skewed by air temperatures well above 0°C (30 dates with air temperature > 4°C, 5 dates with air temperature >8°C), as the snow surface cannot warm above freezing without melting. Removing these dates reduced the temporal coverage of the summer MODIS LST offset data, but had no effect on the seasonal distribution of the apparent bias.

https://doi.org/10.5194/tc-2021-211
Preprint. Discussion started: 27 September 2021

2.3 Sensor footprint size

To test if the LST offset is a result of the MODIS sensor's large footprint, we calculate the difference between ASTER (90 m footprint) surface temperatures and AWS measurements, then compare them to the same difference using MODIS data. ASTER kinetic temperature data (AST08, https://search.earthdata.nasa.gov/search) for 2001-2020 were manually filtered to remove dates with cloud cover or inconsistency in their time of acquisition, resulting in 33 ASTER images coincident with MODIS imagery at Divide, and 15 at Eclipse. The seasonal distribution of acquired ASTER imagery is heavily skewed, with only three images available during winter months and none during spring. While Landsat also has a smaller footprint than MODIS (100-120 m), Landsat surface temperatures remain under development and were therefore not included in this study.

2.4 Snow surface emissivity

To test if the MODIS LST offset is a result of poorly constrained snow emissivity values, we assessed whether the prominent wintertime offset in MODIS LSTs is also present in MODIS brightness temperatures prior to the incorporation of snow surface emissivity. MODIS brightness temperatures (https://lpdaacsvc.cr.usgs.gov/appeears/) were extracted, and their offset from AWS temperatures was calculated. We also examined ASTER and Landsat brightness temperatures because of their higher spatial resolution (90 m for ASTER, 100-120 m for Landsat). ASTER brightness temperatures were obtained from TIR imagery (https://search.earthdata.nasa.gov/search; using the methods of Ndossi and Avdan 2016). Landsat top of atmosphere brightness temperature imagery (https://earthexplorer.usgs.gov/) was manually examined for cloud cover, and cloud-free pixels were extracted for analysis using QGIS.

2.5 Near-surface temperature inversions

To test whether the MODIS LST offset reflects pervasive near-surface temperature inversions, we examine whether the offset is more pronounced under conditions that facilitate near-surface inversions, namely low levels of incoming solar radiation and low wind speeds. Low solar radiation gives rise to near-surface inversions, but it can be counterbalanced if wind speeds are high enough to disturb thermal stratification (Adolph et al., 2018). We compare differences between AWS and MODIS LST data to wind speed and solar radiation data obtained from the Divide AWS.

To test if a near-surface temperature inversion would be physically plausible under surface conditions at Divide and Eclipse, we compare differences in AWS and MODIS temperatures to a theoretical model of temperature inversions.To calculate the theoretical difference between 2 m air and surface temperatures explained by a temperature inversion, we focus on the radiative components of the surface energy balance. The net surface energy balance (E_N) can be expressed by:

$$E_N = E_S\downarrow + E_S\uparrow + E_L\downarrow + E_L\uparrow + E_G + E_H + E_E + E_P \quad (1)$$

where $E_S\downarrow$ is the downward shortwave radiation, $E_S\uparrow$ is the reflected shortwave radiation, $E_L\downarrow$ is the downward longwave radiation, $E_L\uparrow$ is the upward emitted longwave radiation, E_G is the subsurface energy flux, E_H and E_E are the turbulent sensible and latent heat fluxes, and E_P is the heat flux associated with liquid precipitation that subsequently freezes (Cuffey

https://doi.org/10.5194/tc-2021-211
Preprint. Discussion started: 27 September 2021

and Paterson 2010). We focus on the radiative fluxes ($E_S\downarrow$, $E_S\uparrow$, $E_L\downarrow$, and $E_L\uparrow$), as our goal is simply to determine whether observed temperature differences are physically plausible, and not to produce a precise energy balance model. We ignore E_G because it is often small relative to both radiative and turbulent fluxes, and several studies (e.g. Brock and Arnold, 2000; Hock and Noetzli, 1997, Favier et al., 2004) have validated energy models in which it is omitted (Pellicciotti et al., 2009). We also ignore E_P, as rainfall has not been observed in the St. Elias icefields, and turbulent fluxes, as they are difficult to calculate, and unnecessary for our purposes of evaluating the physical plausibility of observed temperature differences. Additionally, LST offsets observed in this study are most prominent under low wind speed conditions, when turbulent fluxes are unlikely to be a dominant component of the surface energy balance. Ignoring turbulent fluxes, we can still calculate an upper bound for temperature inversion strength under site conditions at Divide and Eclipse. After applying our simplifying assumptions, equation 1 becomes:

$$E_N = E_S\downarrow + E_S\uparrow + E_L\downarrow + E_L\uparrow \tag{2}$$

We assume a net surface energy balance of $E_N = 0$. Expressing $E_L\uparrow$ in terms of its components, and rearranging to solve for surface temperature (T_s), we obtain:

$$T_s = \left(\frac{E_L\downarrow + E_S\downarrow(1-\alpha)}{\epsilon_s\sigma}\right)^{0.25} \tag{3}$$

where α is surface albedo, ϵ_s is surface emissivity and σ is the Stefan-Boltzmann constant. We acquire downward shortwave radiation from the Divide AWS. We calculate downward longwave radiation as follows, using 2 m air temperature (T_a) from Divide and atmospheric emissivity (ϵ_a) from the ERA5 reanalysis product:

$$E_L\downarrow = \sigma\epsilon_a {T_a}^4 \tag{4}$$

We use a surface albedo of 0.742, which was the mean albedo measured at Divide during August, 2015 (Williamson et al., 2016). We use end-member snow emissivity values of $\epsilon_s = 0.95$ and $\epsilon_s = 0.99$ (Hori et al., 2006). We assign a value of 0°C to all surface temperatures calculated to be above 0°C because a snow surface cannot exceed this temperature without melting.

3 Results

3.1 Seasonal distribution of the MODIS LST offset

In comparing MODIS LSTs with AWS temperatures at Divide and Eclipse, we find the MODIS LST offset to be greatest during the fall and winter (Table 3). Median differences between AWS temperatures and MODIS LSTs at Divide are larger in the fall (Mdn = -4.43°C) and winter (Mdn = -8.40°C) than in the spring (Mdn = -0.68°C) and summer (Mdn = -0.98°C; Table 2). Winter LST offsets are significantly larger than those in spring (Wilcoxon rank sum test $z = 13.41$, $p < 0.05$), summer (Wilcoxon rank sum test $z = 12.35$, $p < 0.05$), and fall (Wilcoxon rank sum test $z = 5.53$, $p < 0.05$). Fall LST offsets are significantly larger than those in spring (Wilcoxon rank sum test $z = 9.85$, $p < 0.05$) and summer (Wilcoxon rank sum test

https://doi.org/10.5194/tc-2021-211
Preprint. Discussion started: 27 September 2021

The Cryosphere Discussions

Table 3. Results for Wilcoxon rank sum tests between seasonal MODIS LST offsets at Divide (a) and Eclipse (b). Blue cells indicate a more pronounced apparent cold bias in the column season, orange cells indicate a more pronounced apparent cold bias in the row season, and white cells indicate no significant difference between the seasons.

(a)

Divide	Spring (MAM)	Summer (JJA)	Fall (SON)	Winter (DJF)
Spring (MAM)		z = 0.81 p > 0.05	z = 9.85 p < 0.05	z = 13.41 p < 0.05
Summer (JJA)	z = 0.81 p > 0.05		z = 8.80 p < 0.05	z = 12.35 p < 0.05
Fall (SON)	z = 9.85 p < 0.05	z = 8.80 p < 0.05		z = 5.53 p < 0.05
Winter (DJF)	z = 13.41 p < 0.05	z = 12.35 p < 0.05	z = 5.53 p < 0.05	

(b)

Eclipse	Spring (MAM)	Summer (JJA)	Fall (SON)	Winter (DJF)
Spring (MAM)		z = 1.11 p > 0.05	z = 2.62 p < 0.05	z = 3.59 p < 0.05
Summer (JJA)	z = 1.11 p > 0.05		z = 3.73 p < 0.05	z = 4.39 p < 0.05
Fall (SON)	z = 2.62 p < 0.05	z = 3.73 p < 0.05		z = 1.15 p > 0.05
Winter (DJF)	z = 3.59 p < 0.05	z = 4.39 p < 0.05	z = 1.15 p > 0.05	

$z = 8.80$, $p < 0.05$). Differences between AWS temperatures and MODIS LSTs at Eclipse are also larger in the fall (Mdn = -5.20°C) and winter (Mdn = -8.93°C) than in the spring (Mdn = -1.73°C) and summer (Mdn = -1.12°C). Fall and winter LST offsets do not differ significantly from each other in magnitude (Wilcoxon rank sum test $z = 1.15$, $p > 0.05$). Fall LST offsets are significantly larger than those during spring (Wilcoxon rank sum test $z = 2.62$, $p < 0.05$) and summer (Wilcoxon rank sum test $z = 3.73$, $p < 0.05$). Winter LST offsets are likewise significantly larger than those during spring (Wilcoxon rank sum test $z = 3.59$, $p < 0.05$) and summer (Wilcoxon rank sum test $z = 4.39$, $p < 0.05$).

3.2 Sensor footprint size

In comparing MODIS (1 km) and ASTER (90 m) surface temperatures, we find that they both show an offset relative to AWS measurements at Divide, with the MODIS offset (Mdn = -2.90) being significantly smaller than the ASTER offset (Mdn = -6.26; Wilcoxon rank sum test $z = 2.1533$, $p < 0.05$; Fig. 4). In all seasons, the MODIS temperature difference data spans >10°C, with the range of winter values being greatest at 35.56°C at Divide and 25.13°C at Eclipse. No ASTER temperatures were produced coincident with MODIS LSTs during the winter, and only three during the spring so we were unable to bin ASTER data by season. Only one ASTER temperature was produced coincident with MODIS LSTs at Eclipse.

3.3 Snow surface emissivity

In comparing MODIS temperature products before and after the incorporation of snow surface emissivity, MODIS brightness temperatures in bands 31 and 32 (prior to the incorporation of snow emissivity) show similar offset patterns as the LST products (after the incorporation of snow emissivity), with the apparent cold bias being most prominent in fall and winter (Table 2, Table 4, Fig. 5). At Divide, winter offsets across both bands (Mdn = -9.39) are significantly larger than those in spring (Mdn = -1.74, Wilcoxon rank sum test $z = 19.09$, $p < 0.05$), summer (Mdn = -2.43, Wilcoxon rank sum test $z = 16.70$, $p < 0.05$),

https://doi.org/10.5194/tc-2021-211
Preprint. Discussion started: 27 September 2021

The Cryosphere
Discussions
Open Access
EGU

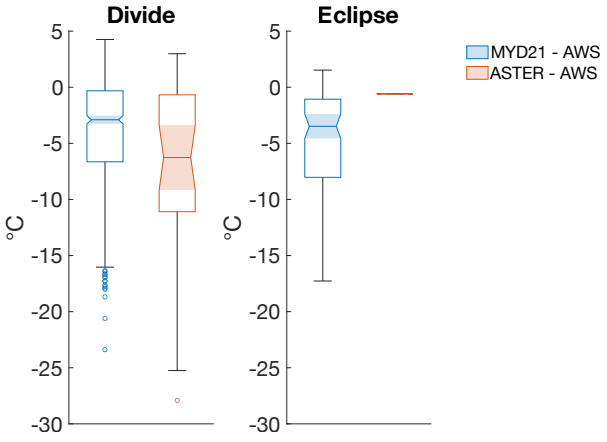

Figure 4. Differences between remote sensing surface temperatures and AWS measurements at Divide and Eclipse. Temperature products from both MODIS (a) and ASTER (b) show an apparent cold bias relative to AWS temperatures. Shaded notched areas indicate the 95% confidence interval for the median temperature difference.

and fall (Mdn = -5.64, Wilcoxon rank sum test $z = 8.63$, $p < 0.05$). Fall offsets are significantly larger than those in spring (Wilcoxon rank sum test $z = 13.39$, $p < 0.05$) and summer (Wilcoxon rank sum test $z = 10.20$, $p < 0.05$). At Eclipse, fall (Mdn = -5.67) and winter (Mdn = -9.41) offsets do not differ significantly from each other in magnitude (Wilcoxon rank sum test $z = 1.77$, $p > 0.05$). Fall offsets are significantly larger than those during spring (Mdn = -2.77, Wilcoxon rank sum test $z = 3.25$, $p < 0.05$) and summer (Mdn = -2.53, Wilcoxon rank sum test $z = 4.57$, $p < 0.05$). Winter offsets are likewise significantly larger than those during spring (Wilcoxon rank sum test $z = 4.70$, $p < 0.05$) and summer (Wilcoxon rank sum test $z = 5.83$, $p < 0.05$).

Landsat brightness temperatures at Divide also show a pattern of greater offset from AWS temperatures in the fall (Mdn = -4.15) and winter (Mdn = -12.11) than in the spring (Mdn = -1.33) and summer (Mdn = -2.65). Winter offsets are significantly larger than those in spring (Wilcoxon rank sum test $z = 5.96$, $p < 0.05$), summer (Wilcoxon rank sum test $z = 5.15$, $p < 0.05$), and fall (Wilcoxon rank sum test $z = 4.30$, $p < 0.05$). Fall offsets are significantly larger than those in spring (Wilcoxon rank sum test $z = 4.88$, $p < 0.05$) and summer (Wilcoxon rank sum test $z = 2.24$, $p < 0.05$).

3.4 Near-surface temperature inversions

Similar to findings at Summit, Greenland (Adolph et al., 2018), the MODIS LST offset in the St. Elias is most pronounced under conditions that facilitate near-surface temperature inversions, namely low wind speeds and low levels of incoming solar radiation (Fig. 6). The magnitude of the offset correlates weakly with wind speed ($r^2 = 0.02$, $p < 0.05$) and more strongly with solar radiation ($r^2 = 0.34$, $p < 0.05$; Fig. 7). Nearly all (97%) MODIS LST offsets in excess of 10°C are coincident with solar radiation lower than 430 W m^{-2}. A majority (95%) of MODIS LST offsets in excess of 10°C are coincident with wind speeds

https://doi.org/10.5194/tc-2021-211
Preprint. Discussion started: 27 September 2021

The Cryosphere Discussions
Open Access
EGU

Table 4. Results for Wilcoxon rank sum tests between seasonal MODIS brightness temperature offsets from AWS temperatures at Divide (a) and Eclipse (b). Brightness temperatures for bands 31 and 32 are averaged together. Blue cells indicate a more pronounced apparent cold bias in the column season, orange cells indicate a more pronounced apparent cold bias in the row season, and white cells indicate no significant difference between the seasons.

(a)

Divide	Spring (MAM)	Summer (JJA)	Fall (SON)	Winter (DJF)
Spring (MAM)		z = 3.60 p < 0.05	z = 13.39 p < 0.05	z = 19.09 p < 0.05
Summer (JJA)	z = 3.60 p < 0.05		z = 10.20 p < 0.05	z = 16.70 p < 0.05
Fall (SON)	z = 13.39 p < 0.05	z = 10.20 p < 0.05		z = 8.63 p < 0.05
Winter (DJF)	z = 19.09 p < 0.05	z = 16.70 p < 0.05	z = 8.63 p < 0.05	

(b)

Eclipse	Spring (MAM)	Summer (JJA)	Fall (SON)	Winter (DJF)
Spring (MAM)		z = 0.95 p > 0.05	z = 3.25 p < 0.05	z = 4.70 p < 0.05
Summer (JJA)	z = 0.95 p > 0.05		z = 4.57 p < 0.05	z = 5.83 p < 0.05
Fall (SON)	z = 3.25 p < 0.05	z = 4.57 p < 0.05		z = 1.77 p > 0.05
Winter (DJF)	z = 4.70 p < 0.05	z = 5.83 p < 0.05	z = 1.77 p > 0.05	

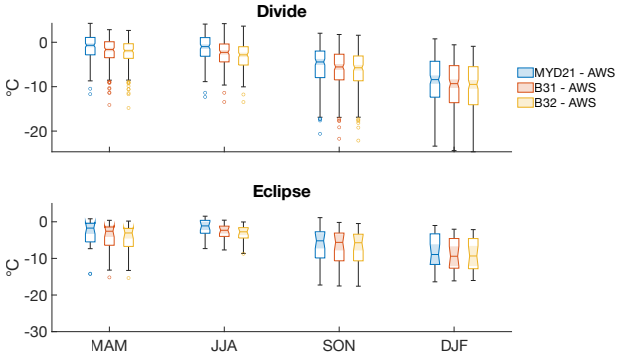

Figure 5. Offsets of MODIS surface temperatures, MODIS Band 31 brightness temperatures and MODIS Band 32 brightness temperatures from AWS measurements at Divide and Eclipse. At Divide, spring and summer apparent cold biases are smaller in the final surface temperatures than in brightness temperatures (95% confidence interval); fall and winter apparent cold biases show no difference between final surface temperatures and brightness temperatures (95% confidence interval). Surface and brightness temperatures show no significant difference from each other at Eclipse in any season due to smaller sample sizes.

lower than 40 $\mathrm{km\,h^{-1}}$. Comparing these findings with modeled results, we find that modeled temperature inversions are also strongest in the winter (Table 5). Modeled surface temperatures show a more pronounced offset from 2 m air temperatures in winter than in spring (Wilcoxon rank sum test $z = 21.81$, $p < 0.05$ for $\epsilon_s = 0.95$), summer (Wilcoxon rank sum test $z = 10.75$, $p < 0.05$ for $\epsilon_s = 0.95$), and fall (Wilcoxon rank sum test $z = 11.82$, $p < 0.05$ for $\epsilon_s = 0.95$). The observed median MODIS LST offset is 8.40°C in the winter and 0.98°C in the summer (Table 2). Our simple energy balance model predicts a median temperature inversion of 4.76°C ($\epsilon_s = 0.95$) and 7.35°C ($\epsilon_s = 0.99$) in the winter, and no inversion in the summer (Fig. 8).

https://doi.org/10.5194/tc-2021-211
Preprint. Discussion started: 27 September 2021

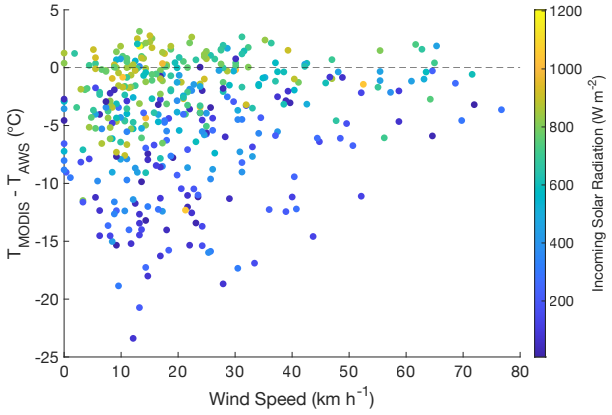

Figure 6. Comparison of the MODIS LST offset (MODIS-AWS) with measured solar radiation and wind speed. The MODIS LSTs show the most pronounced apparent cold bias at low levels of solar radiation (shown by marker color) and low wind speeds. Horizontal dashed line marks all locations where MODIS = AWS.

Table 5. Results for Wilcoxon rank sum tests between modeled temperature inversions by season. Inversions ($T_{surface} - T_{air}$) were calculated from ERA5 and Divide AWS data. Blue cells indicate a larger inversion in the column season, orange cells indicate a larger inversion in the row season, and white cells indicate no significant difference between the seasons.

$\epsilon = 0.95$	Spring (MAM)	Summer (JJA)	Fall (SON)	Winter (DJF)
Spring (MAM)		z = 27.84 p < 0.05	z = 17.41 p < 0.05	z = 21.81 p < 0.05
Summer (JJA)	z = 27.84 p < 0.05		z = 9.95 p < 0.05	z = 10.75 p < 0.05
Fall (SON)	z = 17.41 p < 0.05	z = 9.95 p < 0.05		z = 11.82 p < 0.05
Winter (DJF)	z = 21.81 p < 0.05	z = 10.75 p < 0.05	z = 11.82 p < 0.05	

$\epsilon = 0.99$	Spring (MAM)	Summer (JJA)	Fall (SON)	Winter (DJF)
Spring (MAM)		z = 26.81 p < 0.05	z = 18.76 p < 0.05	z = 23.96 p < 0.05
Summer (JJA)	z = 26.81 p < 0.05		z = 5.62 p < 0.05	z = 15.38 p < 0.05
Fall (SON)	z = 18.76 p < 0.05	z = 5.62 p < 0.05		z = 13.29 p < 0.05
Winter (DJF)	z = 23.96 p < 0.05	z = 15.38 p < 0.05	z = 13.29 p < 0.05	

In the winter, the spread of modeled temperature difference data is greater than 60°C. In the summer, these data show a much narrower spread because of our 0°C cap on surface temperatures. The diurnal surface temperature offset cycle is more pronounced in the summer than in the winter, with the greatest offset occurring during nighttime hours, justifying the decision to limit MODIS LSTs to midday image collection (Fig. 9, Table 6).

https://doi.org/10.5194/tc-2021-211
Preprint. Discussion started: 27 September 2021

The Cryosphere
Discussions
Open Access
EGU

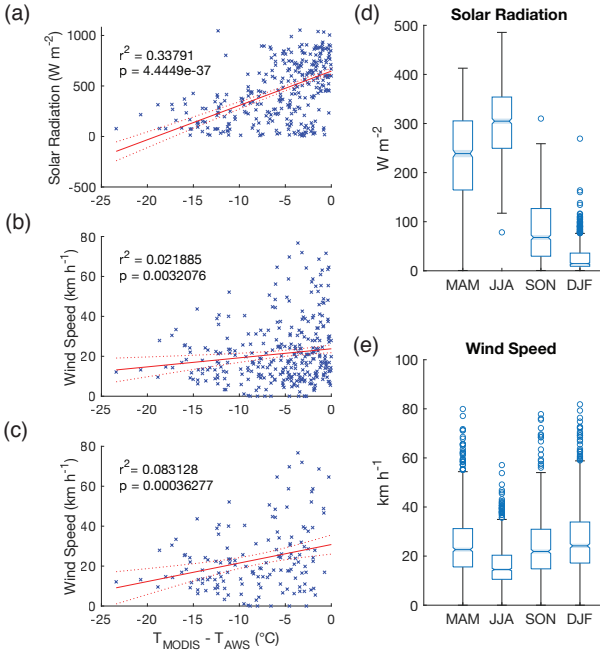

Figure 7. Linear regressions of the MODIS LST offset vs. solar radiation (a), MODIS LST offset vs. wind speed (b), and MODIS LST offset vs. wind speed under low (< 400 $\mathrm{Wm^{-2}}$) solar radiation conditions, and boxplots of solar radiation (d) and wind speed (e) by season. The magnitude of the MODIS LST offset is more strongly related to solar radiation than to wind speed. Dashed red lines in regression plots indicate the 95% confidence interval around the regression line. Notches and shading in boxplots indicate the upper and lower bounds of each season's median value of solar radiation or wind speed at the 95% confidence interval.

4 Discussion

4.1 Sensor footprint size

Despite ASTER's smaller footprint and the homogeneity of surface type within its pixel relative to that within the MODIS pixel, the LST offset persists in ASTER data (Fig. 4). The LST offset in ASTER data indicates that averaging temperature over MODIS' square kilometer footprint alone does not account for the apparent cold bias in MODIS LSTs. Additionally, AWS temperatures at Divide and Eclipse show good coherence, with a mean temperature difference between the sites of 0.93°C $\pm$ 2.00°C, despite the two sites being 30 km apart and over 400 m of elevation difference between them. At its most extreme, the temperature difference measured by weather stations between the two sites reaches ~8°C. Although 8°C is notable, the fact that it is on the upper extreme of temperature disparities over 30 km and 400 m of elevation demonstrates that averaging temperatures over a single square kilometer is unlikely to routinely produce an offset of similar magnitude in wintertime

https://doi.org/10.5194/tc-2021-211
Preprint. Discussion started: 27 September 2021

The Cryosphere Discussions
Open Access
EGU

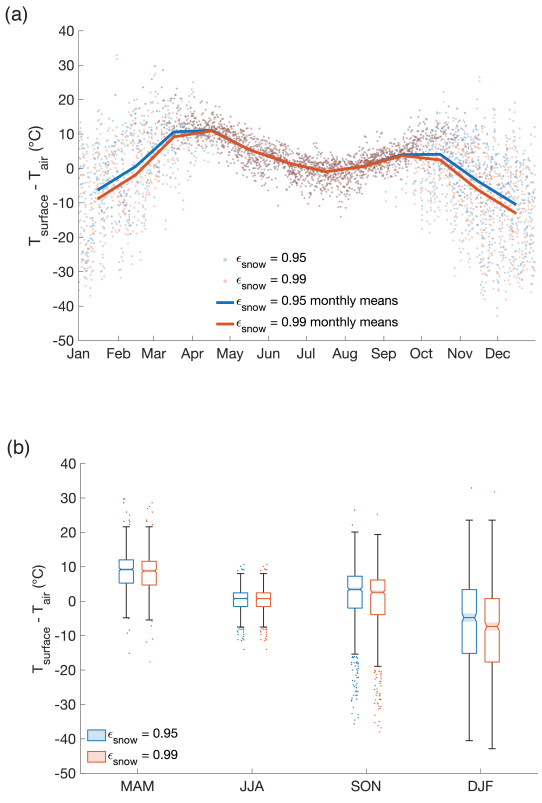

Figure 8. Seasonal differences between surface and 2 m air temperatures calculated from ERA5 and Divide AWS data. All data are for time 12:00 to control for diurnal effects. Shaded notched areas in panel (b) indicate the 95% confidence interval for the median temperature difference. All surface temperatures > 0°C were assigned a value of 0°C.

MODIS LSTs (Mdn = −8.40 at Divide, Mdn = −8.93 at Eclipse). MODIS' footprint size is thus not the dominant source of the offset in its LSTs.

4.2 Snow surface emissivity

In comparing MODIS LSTs with brightness temperatures, which do not include a correction for emissivity, we find that brightness and surface temperatures show a similar seasonal distribution of offset from AWS temperatures, suggesting that poorly constrained emissivity values also fail to account for the entire offset. If the apparent cold bias were introduced prior to the surface temperature conversion, we would expect brightness temperatures to exhibit a greater offset from AWS measurements in the fall and winter than in the spring and summer, similar to the final LST product. If, however, the apparent cold bias were introduced by the emissivity values used in this conversion, we would expect the prominent fall and winter offset to be absent from the MODIS brightness temperatures. MODIS brightness temperatures and surface temperatures do show the same pattern of increased offsets from AWS measurements during the fall and winter (Fig. 5). Moreover, Landsat brightness temperatures

https://doi.org/10.5194/tc-2021-211
Preprint. Discussion started: 27 September 2021

The Cryosphere Discussions
Open Access
EGU

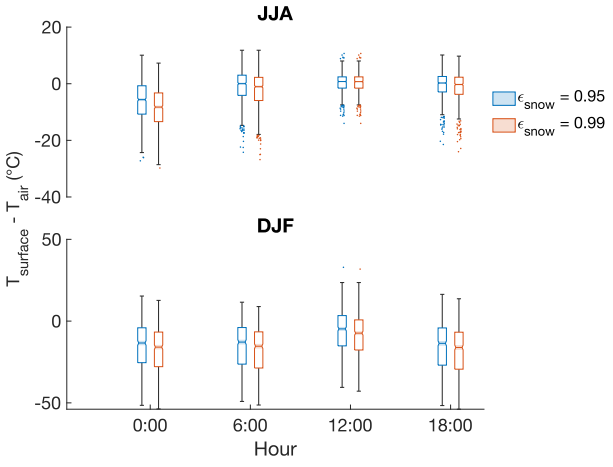

Figure 9. Diurnal differences between surface and 2 m air temperatures calculated from ERA5 and Divide AWS data. Summer (JJA) and winter (DJF) data are shown separately to control for seasonal effects. Shaded notched areas indicate the 95% confidence interval for the median temperature difference. All surface temperatures > 0°C were assigned a value of 0°C.

also show a pattern of greater offset from AWS temperatures in the fall and winter. The observed apparent cold bias in MODIS LSTs is therefore not unique to the MYD21 product or even the MODIS sensor. Unfortunately, due to the limited availability of ASTER data, too few images exist to examine any seasonal pattern.

While results here show that poorly constrained emissivity values do not introduce the apparent cold bias, they may exacerbate it. Applying an accurate emissivity correction to MODIS brightness temperatures should bring the resultant surface temperatures closer to AWS measurements. At Divide, MODIS surface temperatures are ∼60% closer to AWS measurements than MODIS brightness temperatures during spring and summer (significant at the 95% confidence interval, Fig. 5). During the fall and winter, however, there is no significant difference between the median offsets in MODIS brightness and surface temperatures (95% confidence interval), suggesting that emissivity values during these seasons may contribute to the offset in resultant surface temperatures. At Eclipse, the median offset between MODIS LSTs and AWS temperatures does not differ from that between MODIS brightness and AWS temperatures in any season (95% confidence interval). However, Eclipse imagery was limited (20-30 samples per season at Eclipse vs. 169-203 samples per season at Divide), so a robust analysis could not be completed.

Emissivity values may be especially poorly known under winter conditions because of rapidly changing snow surface characteristics, resulting in the seasonal difference in outcome of the LST algorithm as seen at Divide. In particular, the role of emissivity changes following snowfall events requires further examination. Emissivity increases with surface melt, and decreases with increasing particle size and density, which can occur due to either packing or welding of grains as the snow surface evolves following a snowfall event (Salisbury et al., 1994). In the 10.5-12.5 µm wavelength range (MODIS bands 31 and 32), emissivity can vary from 0.949 to 0.997 depending on the surface type (fine dendrite snow, medium granular snow,

https://doi.org/10.5194/tc-2021-211
Preprint. Discussion started: 27 September 2021

Table 6. Results for Wilcoxon rank sum tests between modeled temperature inversions at hours 00:00, 06:00, 12:00, and 18:00 during the summer (a) and winter (b). Inversions ($T_{surface} - T_{air}$) were calculated from ERA5 and Divide AWS data. Blue cells indicate a larger inversion in the column hour, orange cells indicate a larger inversion in the row hour, and white cells indicate no significant difference between the hours.

(a) Summer (JJA)

$\epsilon = 0.95$	00:00	00:06	00:12	00:18
00:00		z = 16.77 p < 0.05	z = 22.04 p < 0.05	z = 18.73 p < 0.05
00:06	z = 16.77 p < 0.05		z = 3.89 p < 0.05	z = 0.71 p > 0.05
00:12	z = 22.04 p < 0.05	z = 3.89 p < 0.05		z = 3.46 p < 0.05
00:18	z = 18.74 p < 0.05	z = 0.71 p > 0.05	z = 3.46 p < 0.05	

$\epsilon = 0.99$	00:00	00:06	00:12	00:18
00:00		z = 19.30 p < 0.05	z = 28.52 p < 0.05	z = 23.48 p < 0.05
00:06	z = 19.30 p < 0.05		z = 8.47 p < 0.05	z = 3.00 p < 0.05
00:12	z = 28.52 p < 0.05	z = 8.47 p < 0.05		z = 6.09 p < 0.05
00:18	z = 23.48 p < 0.05	z = 3.00 p < 0.05	z = 6.09 p < 0.05	

(b) Winter (DJF)

$\epsilon = 0.95$	00:00	00:06	00:12	00:18
00:00		z = 0.14 p > 0.05	z = 10.48 p < 0.05	z = 0.45 p > 0.05
00:06	z = 0.14 p > 0.05		z = 10.70 p < 0.05	z = 0.34 p > 0.05
00:12	z = 10.48 p < 0.05	z = 10.70 p < 0.05		z = 10.85 p < 0.05
00:18	z = 0.45 p > 0.05	z = 0.34 p > 0.05	z = 10.85 p < 0.05	

$\epsilon = 0.99$	00:00	00:06	00:12	00:18
00:00		z = 0.14 p > 0.05	z = 10.46 p < 0.05	z = 0.45 p > 0.05
00:06	z = 0.14 p > 0.05		z = 10.69 p < 0.05	z = 0.34 p > 0.05
00:12	z = 10.46 p < 0.05	z = 10.69 p < 0.05		z = 10.84 p < 0.05
00:18	z = 0.45 p > 0.05	z = 0.34 p > 0.05	z = 10.84 p < 0.05	

coarse grain snow, sun crust, and bare ice), with lower emissivity values for coarse grain snow and ice than for fine dendrite snow (Wan and Zhang, 1999; Hori et al., 2006). To test if the enhanced winter LST offset could result from surface evolution following snowfall events, we compared the Divide snowfall record to the magnitude of the MODIS LST offset. However, given the low temporal resolution of the MODIS data relative to the accumulation record (1 image per day vs. 1 sample per hour), we found no relationship either between the LST offset and individual snowfall events or between the LST offset and the total accumulation, the percent of days with accumulation, or the mean days between accumulation each month. Additional sampling is needed to fully evaluate this relationship.

https://doi.org/10.5194/tc-2021-211
Preprint. Discussion started: 27 September 2021

4.3 Near-surface temperature inversions

Results showing that the MODIS LST offset is highly correlated with the level of solar radiation supports the hypothesis that a near-surface temperature inversion is the primary driver of the observed offset. Incoming solar radiation is lowest in the fall and winter, when the offset is greatest, and therefore may be a root control on the seasonal nature of the apparent cold bias. Low wind speeds maintain existing near-surface inversions; however, solar radiation is the primary control on inversion development, providing an explanation for the weaker correlation between the LST offset and wind speed. Observed wintertime MODIS LSTs show a median offset of greater than 8°C at both Divide and Eclipse (Table 2). Results from the simple energy balance model support these observations, predicting a median wintertime temperature inversion of 4.76°C ($\epsilon_s = 0.95$) and 7.35°C ($\epsilon_s = 0.99$) at divide and eclipse, respectively. However, wintertime near-surface temperature inversions have been observed at other glaciated sites (where both air and surface temperatures have been measured in situ), but with smaller magnitudes than the MODIS LST offset and predicted inversions at Divide and Eclipse. Surface temperatures at the South Pole during the winter of 2001 were a median of 1.3°C lower than 2 m air temperatures under clear sky conditions (Hudson and Brandt, 2005). Likewise, surface temperatures at Summit, Greenland were 1.5 ± 0.2°C lower than 2 m air temperatures during the winter of 2008–2009 (Koenig and Hall, 2010). This discrepancy may be due to a stronger influence of turbulent fluxes at the South Pole and Summit sites or to variations in albedo, as both turbulent fluxes and surface albedo can be strong controls on surface energy balance (Braithwaite and Olesen, 1990; Oerlemans, 1991; Ebrahimi and Marshall, 2016).

In comparing the magnitude of the summer LST offset here (JJA Mdn $= -0.98$°C), to prior studies, the offsets presented here are smaller than previously observed summer MODIS LST offsets in the St. Elias (5–7°C, Williamson et al. 2017). However, these prior LSTs were daily averages of maximum and minimum values, with most of the offset being attributed to the inclusion of minimum LSTs (Williamson et al., 2017). In contrast, this study uses a single daily LST value and coincident AWS measurements acquired between 11:00 a.m. and 1:30 p.m, when surface and air temperatures are near their maximum, thereby eliminating the effects of any diurnal cycle on observed LST offsets. Our modeled temperature inversions show a diurnal cycle, which is more dramatic in the summer than the winter because of the greater difference between incoming solar radiation during the day and night, and is likely responsible for the higher magnitude of the previously observed summer LST offsets (Fig. 9, Table 6). The magnitude of the summer LST offset at Eclipse and Divide is in closer agreement with temperature inversions observed at Summit, Greenland, where 2 m air and surface temperatures have been contemporaneously measured in situ. During June–July 2015, Summit surface temperatures were 0.32 to 2.4°C lower than 2 m air temperatures (Adolph et al., 2018). At three northern Alaska sites, summer clear-sky surface temperatures were higher than corresponding 2 m air temperatures (Barrow and Atqasuk in 2010, and Olitok Point in 2014; (Good, 2016)). Similarly to Greenland and the St. Elias though, the Alaska sites showed surface temperatures dropped relative to 2 m air temperatures in the fall and winter, suggesting that the conditions responsible for the seasonality of the MODIS LST offset are widespread, although other factors may influence its magnitude (Good, 2016).

Results from the simple energy balance model predict no summertime inversion at all, with surface temperatures being a median of 0.77°C ($\epsilon_s = 0.95$) and 0.75°C ($\epsilon_s = 0.99$) higher than 2 m air temperatures for Eclipse and Divide, respectively. The

https://doi.org/10.5194/tc-2021-211
Preprint. Discussion started: 27 September 2021

dip in modeled summer temperature inversions (Fig. 8) is the result of our 0°C surface temperature cap, which is a simplistic numerical correction for unrealistically high summer surface temperatures over 0°C. However, surface temperatures calculated under similar conditions during parts of the spring and fall are also likely to be unrealistically high, despite not exceeding 0°C. We therefore focus on the magnitudes and seasonal patterns of calculated inversions during summer and winter rather than during the shoulder seasons.

Discrepancies between modeled temperature inversions and observed LST offsets likely arise from variations in albedo, which has a strong control on surface energy balance (Oerlemans, 1991; Ebrahimi and Marshall, 2016). We use an albedo value of $\alpha = 0.742$, but albedo values from $\alpha = 0.661$–0.831 have been measured at Divide (Williamson et al., 2016). Using an albedo of $\alpha = 0.661$ and an emissivity of $\epsilon_s = 0.95$, modeled summer surface temperatures are a median of 38.68°C higher than 2m air temperatures prior to applying the 0°C surface temperature cap. Modeled winter surface temperatures are a median of 2.16°C lower than 2m air temperatures. Using an albedo of $\alpha = 0.831$ and an emissivity of $\epsilon_s = 0.95$, modeled summer surface temperatures are a median of 17.18°C higher than 2m air temperatures, and winter surface temperatures are a median of 8.35°C lower than 2m air temperatures. Our albedo value of $\alpha = 0.661$, measured in August when the snow can be relatively dirty, may therefore be an underestimate during parts of the year when debris is more limited.

Additionally, we do not take turbulent fluxes into account in modeled surface temperatures. Turbulent fluxes serve to dismantle inversions, so we interpret modeled temperature differences to represent an upper bound of expected inversion strength. Overall, the uncertainty in albedo and omission of turbulent fluxes in our modeling lead to wide uncertainty in calculated surface temperatures and inversion strength. However, our simplistic approach is sufficient to explore the physical plausibility of near-surface temperature inversions in the St. Elias. Results suggest that near-surface inversions are plausible at Divide and Eclipse and may account for most of the observed offset in MODIS LSTs. To our knowledge, results here provide the first evidence for near-surface temperature inversions in a heterogeneous alpine environment, as well as the first exploration of their seasonal and diurnal signals in such an environment. Future work is essential to understand near-surface thermal processes in these critical regions, and obtaining in situ air and surface temperatures will be critical in validating these results.

4.4 MODIS LSTs and melt

Despite some uncertainty about the exact mechanism for the MODIS offset, and the lack of an accurate physical correction, MODIS LSTs can still shed light on the important question of surface melt and mass balance in the North Pacific, as the offset is relatively minor during the summer melt season (mean = -1.46°C, std = 3.11°C). Surface melt is primarily driven by high air temperatures, which tend to occur under cloudy conditions when no MODIS imagery is available (Walsh and Chapman, 1998). These conditions preferentially exclude MODIS LSTs on high-melt days and render this remote sensing method ineffective for examining individual extreme melt events. However, interannual trends in MODIS LSTs agree well with those in AWS temperatures ($r^2 = 0.23$ and $p < 0.05$; Fig. 10), and applying a simple linear regression ($y = -3.35 + 0.49x$) reconciles the difference between mean annual MODIS LSTs and AWS temperatures, enabling the use of now-corrected MODIS LSTs (mean error of 0.00 $\pm$ 1.77°C) for both qualitative and quantitative applications related to glacier melt and mass balance on annual timescales. We recommend using corrected mean annual MODIS LSTs in conjunction with regional glacier mass

https://doi.org/10.5194/tc-2021-211
Preprint. Discussion started: 27 September 2021

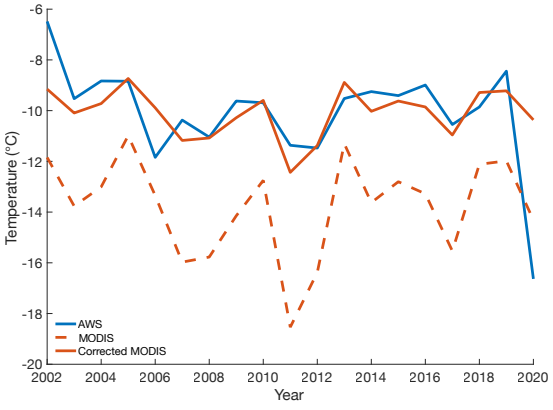

Figure 10. AWS, MODIS, and corrected MODIS mean annual temperatures at Divide. Uncorrected results (dashed orange line) show a prominent apparent cold bias in the remote sensing measurements, but overall agreement in years of high vs. low temperatures. Results corrected by applying a simple linear regression (solid orange line) show much closer agreement with AWS temperatures (solid blue line).

375 balance data to track current temperature changes and glacier response on a broad scale. We also recommend using corrected mean annual MODIS LSTs in the interpretation of refrozen melt archived in ice cores drilled at sites without long in situ temperature records. Qualitatively, MODIS LSTs (corrected or uncorrected) can be used to evaluate whether years of high surface temperatures correspond to years of high amounts of melt in the ice core record. If they do, corrected LSTs can be used to quantitatively describe the relationship between surface temperature and archived melt, enabling the use of refrozen melt as
380 a temperature proxy.

5 Conclusions

Remote sensing is a powerful tool to obtain information about surface conditions at inaccessible locations; however, oftentimes these measurements need calibration and validation. Here we investigated an observed offset in MODIS LSTs from AWS temperatures in the St. Elias Mountains (Yukon, Canada), and found the offset to be most pronounced in the fall and winter.
385 We tested three prominent hypotheses for the origin of the offset: (a) the large spatial footprint of the MODIS sensor in highly heterogeneous alpine terrain, (b) poorly constrained snow emissivity values, and (c) a real temperature difference between the surface and air due to near-surface temperature inversions. We found that the MODIS sensor's large footprint does not account for the offset in its LSTs. Even in highly heterogeneous alpine terrain, the spatial coherence of temperatures across study sites in the region makes it doubtful that offsets from AWS temperatures in excess of 10°C could be regularly obtained
390 by averaging temperature across a single square kilometer to produce the MODIS LST. Moreover, surface temperatures from the ASTER sensor, which has a footprint of 90 m as compared to MODIS' 1 km footprint, still exhibit an offset relative to AWS measurements. Correcting for the MODIS LST offset will therefore require efforts beyond simply improving the spatial resolution of MODIS data. We also found that poorly constrained snow emissivity values fail to account for the MODIS LST

https://doi.org/10.5194/tc-2021-211
Preprint. Discussion started: 27 September 2021

offset; a pronounced fall and winter offset between MODIS brightness temperatures and AWS temperatures is present even prior to the incorporation of snow surface emissivity. However, poorly constrained fall and winter snow emissivity values may exacerbate an existing offset, particularly after snowfall events, when emissivity is likely to change rapidly due to settling and compaction processes. In short, emissivity values are not responsible for the production of the MODIS LST offset, but their role in amplifying it remains unknown.

We found that the physical conditions (low wind speeds, low levels of incoming solar radiation) associated with greater MODIS LST offsets at Eclipse and Divide are consistent with near-surface temperature inversions measured over Greenland (Adolph et al., 2018). In modeling near-surface temperature inversions, we found observed MODIS LST offsets to be within the range of expected inversions based on Divide AWS and ERA5 reanalysis data, supporting the hypothesis that the MODIS LST offset is representative of a physical difference between the properties measured by MODIS (surface temperature) and weather stations (air temperature) rather than the instrumentation or algorithm used to calculate LSTs. Our results provide, to our knowledge, the first evidence for near-surface temperature inversions in a heterogenous alpine environment, indicating that such inversions require continued study to understand surface energy balance in these rapidly changing regions.

Finally, we show that interannual patterns in MODIS LSTs are in good agreement with those of AWS temperature measurements in an alpine environment at Eclipse and Divide. On annual timeframes, we were able to statistically correct for the MODIS LST offset applying a linear correction of $y = -3.35 + 0.49x$. While winter and fall LST offsets remain larger than those in spring and summer, the established correction factor enables a more accurate assessment of melt conditions year to year in alpine environments. This work provides a critical step forward in using remote sensing imagery to expand in situ records and thus provide insight into past and present temperature changes in the St. Elias Mountains and broader North Pacific region.

Author contributions. Ingalise Kindstedt, Kristin M. Schild, and Karl Kreutz formulated the research goals, hypotheses and testing methods. Karl Kreutz, Dominic Winski, Seth Campbell, Luke Copland, and Erin McConnell participated in fieldwork and data collection. Ingalise Kindstedt completed data analysis with contribution from Kristin M. Schild and Dominic Winski. Ingalise Kindstedt prepared the manuscript with contributions from all co-authors.

Competing interests. The authors declare that they have no conflict of interest

Acknowledgements. We thank the National Science Foundation awards #2002483 and #1502783, the National Aeronautics and Space Administration, the Maine Space Grant Consortium, the University of Maine Climate Change Institute, the Canada Foundation for Innovation, Polar Continental Shelf Program, and the Natural Sciences and Engineering Research Council of Canada for support for this work. We thank Icefield Discovery for logistical support, Gerald Holdsworth and Scott Williamson for providing the Eclipse Icefield AWS data, and Christian Zdanowicz and Dorothy K. Hall for additional contributions to data collection.

https://doi.org/10.5194/tc-2021-211
Preprint. Discussion started: 27 September 2021

References

Adolph, A. C., Albert, M. R., and Hall, D. K.: Near-surface temperature inversion during summer at Summit, Greenland, and its relation to MODIS-derived surface temperatures, The Cryosphere, 12, 907–920, https://doi.org/https://doi.org/10.5194/tc-12-907-2018, publisher: Copernicus GmbH, 2018.

Braithwaite, R. J. and Olesen, O. .: A Simple Energy-Balance Model to Calculate Ice Ablation at the Margin of the Greenland Ice Sheet, Journal of Glaciology, 36, 222–228, https://doi.org/10.3189/S0022143000009473, publisher: Cambridge University Press, 1990.

Brock, B. W. and Arnold, N. S.: A spreadsheet-based (Microsoft Excel) point surface energy balance model for glacier and snow melt studies, Earth Surface Processes and Landforms, 25, 649–658, https://doi.org/https://doi.org/10.1002/1096-9837(200006)25:6<649::AID-ESP97>3.0.CO;2-U, _eprint: https://onlinelibrary.wiley.com/doi/pdf/10.1002/1096-9837%28200006%2925%3A6%3C649%3A%3AAID-ESP97%3E3.0.CO%3B2-U, 2000.

Chen, B., Chao, W. C., and Liu, X.: Enhanced climatic warming in the Tibetan Plateau due to doubling CO2: a model study, Climate Dynamics, 20, 401–413, https://doi.org/10.1007/s00382-002-0282-4, 2003.

Cuffey, K. and Paterson, W.: The Physics of Glaciers, Elsevier, Burlington, MA, 4th edn., 2010.

Diaz, H. F., Bradley, R. S., and Ning, L.: Climatic Changes in Mountain Regions of the American Cordillera and the Tropics: Historical Changes and Future Outlook, Arctic, Antarctic, and Alpine Research, 46, 735–743, https://doi.org/10.1657/1938-4246-46.4.735, publisher: Taylor & Francis _eprint: https://doi.org/10.1657/1938-4246-46.4.735, 2014.

Ebrahimi, S. and Marshall, S. J.: Surface energy balance sensitivity to meteorological variability on Haig Glacier, Canadian Rocky Mountains, The Cryosphere, 10, 2799–2819, https://doi.org/10.5194/tc-10-2799-2016, publisher: Copernicus GmbH, 2016.

Farinotti, D., Huss, M., Fürst, J. J., Landmann, J., Machguth, H., Maussion, F., and Pandit, A.: A consensus estimate for the ice thickness distribution of all glaciers on Earth, Nature Geoscience, 12, 168–173, https://doi.org/10.1038/s41561-019-0300-3, number: 3 Publisher: Nature Publishing Group, 2019.

Favier, V., Wagnon, P., Chazarin, J.-P., Maisincho, L., and Coudrain, A.: One-year measurements of surface heat budget on the ablation zone of Antizana Glacier 15, Ecuadorian Andes, Journal of Geophysical Research: Atmospheres, 109, https://doi.org/https://doi.org/10.1029/2003JD004359, _eprint: https://onlinelibrary.wiley.com/doi/pdf/10.1029/2003JD004359, 2004.

Giorgi, F., Hurrell, J. W., Marinucci, M. R., and Beniston, M.: Elevation Dependency of the Surface Climate Change Signal: A Model Study, Journal of Climate, 10, 288–296, https://doi.org/10.1175/1520-0442(1997)010<0288:EDOTSC>2.0.CO;2, publisher: American Meteorological Society, 1997.

Good, E. J.: An in situ-based analysis of the relationship between land surface "skin" and screen-level air temperatures, Journal of Geophysical Research: Atmospheres, 121, 8801–8819, https://doi.org/10.1002/2016JD025318, _eprint: https://agupubs.onlinelibrary.wiley.com/doi/pdf/10.1002/2016JD025318, 2016.

Hill, T., Dow, C. F., Bash, E. A., and Copland, L.: Application of an improved surface energy balance model to two large valley glaciers in the St. Elias Mountains, Yukon, Journal of Glaciology, 67, 297–312, https://doi.org/10.1017/jog.2020.106, publisher: Cambridge University Press, 2021.

Hock, R. and Noetzli, C.: Areal melt and discharge modelling of Storglaciären, Sweden, Annals of Glaciology, 24, 211–216, https://doi.org/10.3189/S0260305500012192, publisher: Cambridge University Press, 1997.

Hori, M., Aoki, T., Tanikawa, T., Motoyoshi, H., Hachikubo, A., Sugiura, K., Yasunari, T. J., Eide, H., Storvold, R., Nakajima, Y., and Takahashi, F.: In-situ measured spectral directional emissivity of snow and ice in the 8–14 μm atmospheric window, Remote Sensing of Environment, 100, 486–502, https://doi.org/10.1016/j.rse.2005.11.001, 2006.

Hudson, S. R. and Brandt, R. E.: A Look at the Surface-Based Temperature Inversion on the Antarctic Plateau, Journal of Climate, 18, 1673–1696, https://doi.org/10.1175/JCLI3360.1, publisher: American Meteorological Society, 2005.

Hugonnet, R., McNabb, R., Berthier, E., Menounos, B., Nuth, C., Girod, L., Farinotti, D., Huss, M., Dussaillant, I., Brun, F., and Kääb, A.: Accelerated global glacier mass loss in the early twenty-first century, Nature, 592, 726–731, https://doi.org/10.1038/s41586-021-03436-z, number: 7856 Publisher: Nature Publishing Group, 2021.

Hulley, G.: MOD21A1D MODIS/Terra Land Surface Temperature/3-Band Emissivity Daily L3 Global 1 km SIN Grid Day V006, https://doi.org/10.5067/MODIS/MOD21A1D.006, type: dataset, 2017.

Hulley, G., Veraverbeke, S., and Hook, S.: Thermal-based techniques for land cover change detection using a new dynamic MODIS multispectral emissivity product (MOD21), Remote Sensing of Environment, 140, 755–765, https://doi.org/10.1016/j.rse.2013.10.014, 2014.

Jin, M. and Dickinson, R. E.: Land surface skin temperature climatology: benefitting from the strengths of satellite observations, Environmental Research Letters, 5, 044 004, https://doi.org/10.1088/1748-9326/5/4/044004, publisher: IOP Publishing, 2010.

Koenig, L. S. and Hall, D. K.: Comparison of satellite, thermochron and air temperatures at Summit, Greenland, during the winter of 2008/09, Journal of Glaciology, 56, 735–741, https://doi.org/10.3189/002214310793146269, publisher: Cambridge University Press, 2010.

Li, H., Li, R., Yang, Y., Cao, B., Bian, Z., Hu, T., Du, Y., Sun, L., and Liu, Q.: Temperature-Based and Radiance-Based Validation of the Collection 6 MYD11 and MYD21 Land Surface Temperature Products Over Barren Surfaces in Northwestern China, IEEE Transactions on Geoscience and Remote Sensing, pp. 1–14, https://doi.org/10.1109/TGRS.2020.2998945, conference Name: IEEE Transactions on Geoscience and Remote Sensing, 2020.

McConnell, E. A.: Mechanisms of Ice Core Stable Isotope Variability in the Upper Kaskawulsh-Donjek Region, St. Elias Mountains, Yukon, Canada, Ph.D. thesis, The University of Maine, https://digitalcommons.library.umaine.edu/etd/3069, 2019.

Ndossi, M. I. and Avdan, U.: Inversion of Land Surface Temperature (LST) Using Terra ASTER Data: A Comparison of Three Algorithms, Remote Sensing, 8, 993, https://doi.org/10.3390/rs8120993, number: 12 Publisher: Multidisciplinary Digital Publishing Institute, 2016.

Oerlemans, J.: A Model for the Surface Balance of Ice Masses: part 1: Alpine Glaciers, Zeitschrift für Gletscherkunde und Glazialgeologie, 27, 63–83, 1991.

Pellicciotti, F., Carenzo, M., Helbing, J., Rimkus, S., and Burlando, P.: On the role of subsurface heat conduction in glacier energy-balance modelling, Annals of Glaciology, 50, 16–24, https://doi.org/10.3189/172756409787769555, publisher: Cambridge University Press, 2009.

Pepin, N., Bradley, R. S., Diaz, H. F., Baraer, M., Caceres, E. B., Forsythe, N., Fowler, H., Greenwood, G., Hashmi, M. Z., Liu, X. D., Miller, J. R., Ning, L., Ohmura, A., Palazzi, E., Rangwala, I., Schöner, W., Severskiy, I., Shahgedanova, M., Wang, M. B., Williamson, S. N., Yang, D. Q., and Mountain Research Initiative EDW Working Group: Elevation-dependent warming in mountain regions of the world, Nature Climate Change, 5, 424–430, https://doi.org/10.1038/nclimate2563, number: 5 Publisher: Nature Publishing Group, 2015.

Rangwala, I. and Miller, J. R.: Climate change in mountains: a review of elevation-dependent warming and its possible causes, Climatic Change, 114, 527–547, https://doi.org/10.1007/s10584-012-0419-3, 2012.

Salisbury, J. W., D'Aria, D. M., and Wald, A.: Measurements of thermal infrared spectral reflectance of frost, snow, and ice, Journal of Geophysical Research: Solid Earth, 99, 24 235–24 240, https://doi.org/10.1029/94JB00579, _eprint: https://agupubs.onlinelibrary.wiley.com/doi/pdf/10.1029/94JB00579, 1994.

Serreze, M. C. and Barry, R. G.: Processes and impacts of Arctic amplification: A research synthesis, Global and Planetary Change, 77, 85–96, https://doi.org/10.1016/j.gloplacha.2011.03.004, 2011.

Shea, C. and Jamieson, B.: Some fundamentals of handheld snow surface thermography, The Cryosphere, 5, 55–66, https://doi.org/https://doi.org/10.5194/tc-5-55-2011, publisher: Copernicus GmbH, 2011.

Shuman, C. A., Hall, D. K., DiGirolamo, N. E., Mefford, T. K., and Schnaubelt, M. J.: Comparison of Near-Surface Air Temperatures and MODIS Ice-Surface Temperatures at Summit, Greenland (2008–13), Journal of Applied Meteorology and Climatology, 53, 2171–2180, https://doi.org/10.1175/JAMC-D-14-0023.1, publisher: American Meteorological Society, 2014.

Walsh, J. E. and Chapman, W. L.: Arctic Cloud–Radiation–Temperature Associations in Observational Data and Atmospheric Reanalyses, Journal of Climate, 11, 3030–3045, https://doi.org/10.1175/1520-0442(1998)011<3030:ACRTAI>2.0.CO;2, publisher: American Meteorological Society Section: Journal of Climate, 1998.

Wan, Z. and Zhang, Y.: MODIS UCSB Emissivity Library, https://icess.eri.ucsb.edu/modis/EMIS/html/em.html, 1999.

Westermann, S., Langer, M., and Boike, J.: Systematic bias of average winter-time land surface temperatures inferred from MODIS at a site on Svalbard, Norway, Remote Sensing of Environment, 118, 162–167, https://doi.org/10.1016/j.rse.2011.10.025, 2012.

Williamson, S. N., Copland, L., and Hik, D. S.: The accuracy of satellite-derived albedo for northern alpine and glaciated land covers, Polar Science, 10, 262–269, https://doi.org/10.1016/j.polar.2016.06.006, 2016.

Williamson, S. N., Hik, D. S., Gamon, J. A., Jarosch, A. H., Anslow, F. S., Clarke, G. K. C., and Scott Rupp, T.: Spring and summer monthly MODIS LST is inherently biased compared to air temperature in snow covered sub-Arctic mountains, Remote Sensing of Environment, 189, 14–24, https://doi.org/10.1016/j.rse.2016.11.009, 2017.

Williamson, S. N., Zdanowicz, C., Anslow, F. S., Clarke, G. K. C., Copland, L., Danby, R. K., Flowers, G. E., Holdsworth, G., Jarosch, A. H., and Hik, D. S.: Evidence for elevation-dependent warming in the St. Elias Mountains, Yukon, Canada, Journal of Climate, https://doi.org/10.1175/JCLI-D-19-0405.1, 2020.

Winski, D., Osterberg, E., Kreutz, K., Wake, C., Ferris, D., Campbell, S., Baum, M., Bailey, A., Birkel, S., Introne, D., and Handley, M.: A 400-Year Ice Core Melt Layer Record of Summertime Warming in the Alaska Range, Journal of Geophysical Research: Atmospheres, 123, 3594–3611, https://doi.org/10.1002/2017JD027539, 2018.

Winton, M.: Amplified Arctic climate change: What does surface albedo feedback have to do with it?, Geophysical Research Letters, 33, https://doi.org/https://doi.org/10.1029/2005GL025244, _eprint: https://onlinelibrary.wiley.com/doi/pdf/10.1029/2005GL025244, 2006.

Yao, R., Wang, L., Wang, S., Wang, L., Wei, J., Li, J., and Yu, D.: A detailed comparison of MYD11 and MYD21 land surface temperature products in mainland China, International Journal of Digital Earth, 0, 1–17, https://doi.org/10.1080/17538947.2019.1711211, publisher: Taylor & Francis _eprint: https://doi.org/10.1080/17538947.2019.1711211, 2020.

You, Q., Cai, Z., Pepin, N., Chen, D., Ahrens, B., Jiang, Z., Wu, F., Kang, S., Zhang, R., Wu, T., Wang, P., Li, M., Zuo, Z., Gao, Y., Zhai, P., and Zhang, Y.: Warming amplification over the Arctic Pole and Third Pole: Trends, mechanisms and consequences, Earth-Science Reviews, 217, 103 625, https://doi.org/10.1016/j.earscirev.2021.103625, 2021.

Zemp, M., Huss, M., Thibert, E., Eckert, N., McNabb, R., Huber, J., Barandun, M., Machguth, H., Nussbaumer, S. U., Gärtner-Roer, I., Thomson, L., Paul, F., Maussion, F., Kutuzov, S., and Cogley, J. G.: Global glacier mass changes and their contributions to sea-level rise from 1961 to 2016, Nature, 568, 382–386, https://doi.org/10.1038/s41586-019-1071-0, number: 7752 Publisher: Nature Publishing Group, 2019.

Østby, T. I., Schuler, T. V., and Westermann, S.: Severe cloud contamination of MODIS Land Surface Temperatures over an Arctic ice cap, Svalbard, Remote Sensing of Environment, 142, 95–102, https://doi.org/10.1016/j.rse.2013.11.005, 2014.